

## Anaerobic digestion of biosolid pyrolysis liquid and hydrolyzed sludge - simulation with extended ADM1 model

Thea Lucia Indrebø\*, Gudny Øyre Flatabø, Wenche Hennie Bergland, Gamunu Samarakoon Arachchige

Department of Process, Energy and Environmental Technology, University of South-Eastern Norway, Kjølnes ring 56, 3918 Porsgrunn, Norway

\*Corresponding author (e-mail: [Thea.L.Indrebo@usn.no](mailto:Thea.L.Indrebo@usn.no))

---

**Abstract:** Pyrolysis of biosolids aims to reduce solid volumes and improve energy recovery; however, the pyrolysis liquid (PL) is a by-product that has no good direct application. One idea is to link pyrolysis and anaerobic digestion (AD), in which PL can be valorized for methane production. PL contains various compounds that potentially threaten the stability of AD. This study, therefore, aims to extend the current Anaerobic Digestion Model No.1 (ADM1) and evaluate the influence of phenol, furfural, 5-hydroxymethylfurfural (5-HMF), styrene, and ammonia from PL on AD. Two lab-scale AD reactors were simulated and compared with experimental data: one fed with hydrolyzed sludge and the other fed with an additional stream of PL. The simulation accurately predicts hydrolyzed sludge as substrate, while the simulation of the reactor co-digesting hydrolyzed sludge and PL overestimates methane production. Ammonia, phenol, and styrene were identified as the most significant inhibitors. However, based on the overestimation of methane production, it is clear that the PL has more inhibitors present than those implemented in the model. Simulations further showed that an additional stream of PL increased methane production by 4.3%, even with significant inhibition by the compounds.

*Keywords:* Pyrolysis Liquid, Anaerobic Digestion, ADM1, Inhibition, Phenol, Ammonia, Styrene, Hydrolyzed Sludge, Biosolids

---

### 1. INTRODUCTION

There is a need for waste management systems which address the world's growing population's energy demand and treat the enormous amount of waste produced in both an efficient and sustainable way (Tayibi et al., 2021). In recent years, coupling pyrolysis and anaerobic digestion (AD) as a waste management system has gained attention due to its possibility for energy recovery and economic value (Feng and Lin, 2017). Pyrolysis is a thermochemical process where organic matter is heated in the absence of oxygen to yield biochar and pyrolysis gas, where pyrolysis liquid (PL) is a by-product. Meanwhile, AD is the biochemical process in which organics biologically degrade to biogas, a mixture of methane and carbon dioxide. Hydrolysis is a rate-limiting step in the AD process, where organic matter is solubilized. Pretreatment methods such as the thermal hydrolysis process (THP) improve hydrolysis with the additional benefits of pathogens removal and enhanced digestate dewaterability (Han et al., 2017).

Pyrolysis coupled with AD offers numerous synergies such as increased resource use by feeding biosolid-PL (PL from dried digestate), biomethanation of pyrolysis gas, and biochar for inhibition control and increased methane production (Tayibi et al., 2021). PL is a by-product of pyrolysis with no direct application and is a complex mixture of more than 400 organics and inorganics (Giwa et al., 2019). Valorization of PL might be possible with AD, but the compounds in PL, such as phenols, furans derivatives, styrene, and ammonia, can inhibit and pose a threat to AD stability (Seyedi et al., 2019). There

have been a few attempts to add PL to AD with an increase in methane production at low PL loadings (Hubner and Mumme, 2015; Seyedi et al., 2020).

Anaerobic Digestion Model nr.1 (ADM1) is a valuable and cost-effective simulation model for predicting an AD system's robustness and efficiency (Batstone et al., 2002). A simulation allows one to anticipate challenges such as inhibition before they arise in the system and predict the outcomes and implications of substrates and substrate combinations. Some previous simulation studies have focused on adding PL to AD. Raya et al. (2021) presented a simulation focusing on how phenol, furfural, and 5-hydroxymethylfurfural (5-HMF) from aqueous-PL from softwood affected AD. Flatabø and Bergland (2022) simulated a full-scale reactor co-digesting sludge from THP, biosolids-PL, and pyrolysis gas. Some studies have focused on the simulation of furfural inhibition from steam explosion pulping wastewater (Li et al., 2023) and phenol simulation from olive mill waste in AD (Fezzani and Ben Cheikh, 2009).

Flatabø and Bergland (2022) only simulated ammonia toxicity, one of many inhibitors in the PL, but neglected the influence of other compounds. This study aims to extend the ADM1 model to predict inhibition from multiple compounds in the PL and evaluate the effects of PL in AD. The objective of this study is to (i) establish an extended model with inhibiting compounds in PL co-digested with sludge from THP and compare the model data to experimental data, (ii) investigate

which compounds contribute to inhibition, and (iii) evaluate the effect of biosolid-PL in AD.

## 2. METHODOLOGY

### 2.1 Anaerobic Digestion System

Substrate consisting of sewage sludge and food waste (60:40 v/v) was collected after treatment in a THP at 155°C with a retention time of 20 minutes. The substrate is termed hydrolyzed sludge (HS) and is the substrate for two lab-scale mesophilic (38°C) semi-continuously stirred tank reactors (semi-CSTRs). Inoculum was sampled from an industrial mesophilic CSTR fed by the same substrate. One AD bioreactor was used as a control and fed HS termed "HS-reactor", while the other was fed HS and PL termed "HSPL-reactor". The PL was produced using the Biogreen® technology by VOW ASA, where dry pelletized biosolids from the industrial CSTR digestate were pyrolyzed at 600°C. More details about the pyrolysis process and PL sampling can be found in Flatabø et al. (2023).

### 2.2 Analytical Characteristics

Total COD (tCOD), soluble COD (sCOD), pH, alkalinity, total ammonia nitrogen (TAN), and volatile fatty acids (VFAs) were analyzed as previously described by Bergland et al. (2015). TAN, pH, and VFAs were analyzed in addition to elemental analysis for the PL; check Flatabø and Bergland (2022) for details. The concentration of phenols in the PL was determined with Supelco Phenol-Test Art.100856 after the sample was filtered (0.45 µm).

### 2.3 Base Case Scenario and Data Collection

The simulations of the lab-scale reactors were implemented in ADM1 in aquasim version 2.1. Both reactors were fed with the same amount of HS, but one was fed with an additional stream of PL. Digestate measurements and characterization were done 1-2 times a week. Both reactors started with only HS as substrate, while the start of the simulation on day 0 was when the HSPL-reactor received PL. More details on the experimental part of the setup can be found in Flatabø et al. (2024). The HS reactor was simulated for 232 days (stopped early due to technical issues). The HSPL-reactor was simulated for 437 days, which was the entire period during which the reactor was fed PL.

### 2.4 Hydrolyzed Sludge (HS) Composition

Average experimental data and literature data were used to simulate both reactors. Both reactors experienced variations in inflow and concentration, and experimental effluent data was used to evaluate the accuracy of the model. The HSPL-reactor had a slightly higher inflow due to the addition of PL, resulting in a lower hydraulic retention time (HRT) than the HS-reactor.

The COD concentration of HS was, on average, 101.1 kg tCOD/m<sup>3</sup> and 21.6 kg sCOD/m<sup>3</sup> at a TS of 5.5-10.8%; a more detailed composition is given in Tab. 1. VFAs were additional inputs and were based on experimental data. Sugars denotes the concentration of n-caproic acid, isocaproic acid and heptanoic acid. Amounts of soluble inert were estimated from effluent data (36.6% of sCOD), while the total inert was

estimated on lab data (COD reduction) and data from the industrial plant (average yield), which on average estimates that 25% of tCOD is inert. For the HSPL-reactor, the total inerts were adjusted to 30% of tCOD after 248 days because of changes in the substrate. Protein composition was set to 9 % of tCOD and lipids to 28% of tCOD based on data from Flatabø and Bergland (2022). Carbohydrates were used to achieve the summed total concentration of COD. The inorganic carbon was based on experimental data. To account for the high pH in the lab experiment, the cations were adjusted in the model by adding 0.15 M in the HS-reactor and 0.2 M in the HSPL-reactor to reach the targeted pH.

**Table 1: Average input data for the hydrolyzed sludge (HS) with a tCOD of 101.1 kg COD/m<sup>3</sup> and sCOD of 21.6 kg COD/m<sup>3</sup>. Lipids, carbohydrates, and proteins were based on data from Flatabø and Bergland (2022), while the other input data were estimated on experimental data.**

Input	Unit	Value
Lipids	kg COD/m <sup>3</sup>	28.6
Carbohydrates	kg COD/m <sup>3</sup>	16.6
Protein	kg COD/m <sup>3</sup>	9.1
Sugars	kg COD/m <sup>3</sup>	0.44
Acetic acid	kg COD/m <sup>3</sup>	1.35
Propionic acid	kg COD/m <sup>3</sup>	0.43
Butyric acid	kg COD/m <sup>3</sup>	0.85
Valeric acid	kg COD/m <sup>3</sup>	1.1
Inert soluble	kg COD/m <sup>3</sup>	7.9
Inert particulate	kg COD/m <sup>3</sup>	26.8
TAN	kmol N/m <sup>3</sup>	0.09
Inorganic carbon	kmol HCO <sub>3</sub> <sup>-</sup> /m <sup>3</sup>	0.03

### 2.4 Pyrolysis Liquid (PL) Composition

The PL composition was obtained from experimental data and literature (see Tab. 2). tCOD and sCOD add up to 355 kg/m<sup>3</sup> and 164 kg/m<sup>3</sup>, respectively. 60% of tCOD is totally inert, in accordance with what Flatabø and Bergland (2022) estimated. The concentration of phenols, 5-HMF, furfural, and styrene are assumed to be soluble in the liquid phase and account for a part of the inert concentration. The 5-HMF and furfural concentrations were found in Hubner and Mumme (2015). Meanwhile, the styrene concentration (0.06 wt.%) is found in Seyedi et al. (2019).

### 2.5 Parameters in the modified ADM1

The hydrolysis constant,  $k_{hyd}$ , was determined to be 1 d<sup>-1</sup> for carbohydrates, lipids, and proteins for HS, which is in accordance with Flatabø and Bergland (2022) and Souza et al., 2013b). For the PL, the hydrolysis constant was determined to be 0.3 d<sup>-1</sup>, as described by Flatabø and Bergland (2022). The disintegration constant was kept at 0.5 d<sup>-1</sup> in

accordance with Montecchio et al. (2017) and Flatabø and Bergland (2022).

**Table 2: Input data for biosolid pyrolysis liquid obtained at a process temperature of 600 °C. The concentrations are 355 kg tCOD/m<sup>3</sup> and 164 kg sCOD/m<sup>3</sup>.**

Input	Unit	Value
Lipids	kg COD/m <sup>3</sup>	37.4 <sup>a</sup>
Carbohydrates	kg COD/m <sup>3</sup>	9.53 <sup>a</sup>
Protein	kg COD/m <sup>3</sup>	7.66 <sup>a</sup>
Sugars	kg COD/m <sup>3</sup>	18.1 <sup>a</sup>
Acetic acid	kg COD/m <sup>3</sup>	40.6 <sup>a</sup>
Propionic acid	kg COD/m <sup>3</sup>	9.45 <sup>a</sup>
Butyric acid	kg COD/m <sup>3</sup>	10.3 <sup>a</sup>
Valeric acid	kg COD/m <sup>3</sup>	8.23 <sup>a</sup>
Inert soluble	kg COD/m <sup>3</sup>	64.8 <sup>a</sup>
Inert particulate	kg COD/m <sup>3</sup>	136 <sup>a</sup>
Phenols	kg COD/m <sup>3</sup>	10.2 <sup>b</sup>
HMF	kg COD/m <sup>3</sup>	0.003 <sup>c</sup>
Furfural	kg COD/m <sup>3</sup>	0.37 <sup>5</sup>
Styrene	kg COD/m <sup>3</sup>	1.84 <sup>d</sup>
TAN	kmol N/m <sup>3</sup>	1.09 <sup>a</sup>
Inorganic carbon	kmol HCO <sub>3</sub> <sup>-</sup> /m <sup>3</sup>	0.313 <sup>b</sup>

Phenol, furfural, 5-HMF, and styrene were extended in the ADM1 to describe the inhibition of PL in AD by using a non-competitive form of inhibition control. Kinetic growth parameters of the phenol in AD were collected from Fezzani and Ben Cheikh (2009), where it is assumed that phenols degrade to hydrogen and benzoate. Inhibition data of phenol was taken from Raya et al. (2021). Phenol and benzoate are included in the charge balance equation to determine pH, as Fezzani and Ben Cheikh (2009) described. Kinetic parameters and inhibition data for furfural degradation are taken from Raya et al. (2021) and Li et al. (2023), where the latter made an extended ADM1 model which took account of the intermediate product furoic acid. Furoic acid is less inhibitory than its precursor, and therefore, inhibition from furoic acid was neglected. Data for growth kinetics and inhibition of 5-HMF in AD was collected from Raya et al. (2021) and B. Liu et al. (2017). For styrene, the inhibition constant,  $K_i$ , on anaerobic mix culture was 145 mg/L (Araya et al., 2000). Anaerobes release 4 units acetic acid and 4 units of hydrogen

<sup>a</sup> Flatabø and Bergland (2022)

<sup>b</sup> Experimental data

for each unit of styrene; thus, the yield of each compound is calculated by (1) and (2).

$$f_{ac,styr} = (1 - Y_{styr}) \cdot \frac{thCOD_{ac} \cdot 4}{thCOD_{ac} \cdot 4 + thCOD_{h2} \cdot 4} \quad (1)$$

$$f_{h2,styr} = (1 - Y_{styr}) \cdot \frac{thCOD_{h2} \cdot 4}{thCOD_{ac} \cdot 4 + thCOD_{h2} \cdot 4} \quad (2)$$

Growth kinetics of styrene degradation under anaerobic conditions is scarce; however, some microbes have been identified to degrade styrene, such as *Pseudomonas sp. E-934846*, which can survive in both anaerobic and aerobic environments (Arnold et al., 1997). Growth kinetics of *Pseudomonas sp. E-934846* on styrene degradation in Gąszczak et al. (2012), where  $k_m$  and  $K_S$  were measured to be 3.96 d<sup>-1</sup> and 0.018 kg COD<sub>s</sub>/m<sup>3</sup>.  $Y$  and  $K_{dec}$  are assumed to be 0.01 and 0.02.

Tab. 3 summarizes the kinetics and values of phenol, benzoate, styrene, 5-HMF, furfural, and furoic acid degradation. For ammonia, default data from ADM1 are used, where  $K_i$  is 0.018 M.

### 3. RESULTS AND DISCUSSION

#### 3.1 Hydrolyzed Sludge Reactor

The experimental and simulated methane productions are shown in Fig. 1.

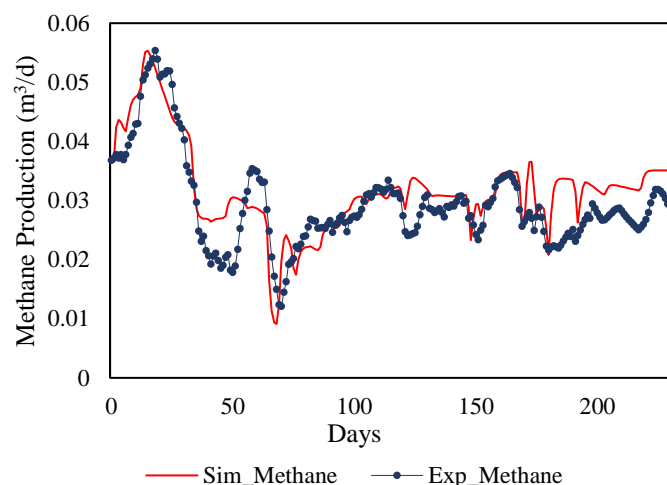


Fig. 1. Experimental (blue dots) and simulated (red line) methane production of reactor only treating hydrolyzed sludge (HS).

Experimental methane production is based on an average COD reduction of 1 week. The model follows experimental values well but overestimates methane production from day 37 to 56 due to changes in inflow in the experiment. After those days, the model predicts methane production well until day 181. The reason for this overestimation after day 181 is unclear. However, according to experimental data, the methane yield

<sup>c</sup> Hubner and Mumme (2015)

<sup>d</sup> Seyedi et al. (2019)

showed a decreasing trend, which is due to the substrate variations that were not accounted for in the model.

The methane partial pressure in the biogas is 63.3% based on simulated values, the same as the previously reported data from Flatabø and Bergland (2022). The pH was slightly lower in the simulation (7.6) than in the experimental results, an average of 7.73. Moreover, the inhibition and inorganic nitrogen concentration are shown in Fig. 2. Simulated TAN and free ammonia (NH<sub>3</sub>) are well predicted compared to experimental data; besides the first 40 days, the simulated values are slightly overestimated. Overestimations of TAN can be due to variations in the substrate composition or the fact that the model is not robust enough to compute accurate data for the first days (Souza et al., 2013b). The main contributor to inhibition is NH<sub>3</sub>, which is 0.3 on average on a scale where 0 is full inhibition and 1 is no inhibition. In the initial days, NH<sub>3</sub> was higher in experimental data compared to

simulated data. Thus, the simulated methane production should probably be more inhibited by NH<sub>3</sub> than what the simulation shows.

### 3.2 Hydrolyzed Sludge and Pyrolysis Liquid Reactor

Simulated and experimental data (based on an average COD reduction for one week) for methane production and PL loading are plotted in Fig. 3. Methane production was underestimated from day 24 to 34 and was overestimated in the next 30 days when the reactor was fed with a reduced flow rate due to operational issues. The simulated values predict the experimental values much better after 266 days, where the PL loading is less than 0.01 L/d (0.14 kg tCOD/m<sup>3</sup>/d) and with long HRTs of 48.6 days compared to the 16.2 and 32.4 days in other periods.

**Table 3: Summary of kinetic parameters of phenol, benzoate, styrene, 5-HMF, furfural, and furoic acid degradation. COD<sub>s</sub> and COD<sub>x</sub> denoted substrate COD and biomass COD, respectively. f indicates the fraction of the compound that converts to another compound.**

Parameter	Description	Unit	Phenol	Benzoate	Furfural	Furoic acid	5-HMF	Styrene	Value
C	Carbon content	kmole/kg COD	0.0268 <sup>a</sup>	0.0324 <sup>a</sup>	0.0284 <sup>a</sup>	0.0347 <sup>a</sup>	0.0312 <sup>a</sup>	0.025 <sup>a</sup>	
k <sub>m</sub>	Maximum uptake rate	d <sup>-1</sup>	15 <sup>b</sup>	8 <sup>b</sup>	20.53 <sup>d</sup>	3.71 <sup>d</sup>	10 <sup>e</sup>	3.96 <sup>h</sup>	
K <sub>s</sub>	Half saturation constant for uptake	kg COD <sub>s</sub> /m <sup>3</sup>	30 <sup>b</sup>	15.5 <sup>b</sup>	9.59 <sup>d</sup>	18.24 <sup>d</sup>	10 <sup>e</sup>	0.018 <sup>h</sup>	
Y	Yield of biomass uptake	kg COD <sub>x</sub> /kg COD <sub>s</sub>	0.01 <sup>b</sup>	0.013 <sup>b</sup>	0.08 <sup>g</sup>	0.08 <sup>a</sup>	0.1 <sup>e</sup>	0.01 <sup>a</sup>	
K <sub>i</sub>	Inhibition on methanogens		1.12 <sup>c</sup>		2.47 <sup>d</sup>		2.05 <sup>c</sup>	0.45 <sup>f</sup>	
K <sub>dec</sub>	Biomass decay rate		0.02 <sup>b</sup>		0.02 <sup>c,g</sup>	0.02 <sup>a</sup>	0.01 <sup>e</sup>	0.02 <sup>a</sup>	
K <sub>i_bnz_h2</sub>	Inhibition on benzoate degraders			9.5·10 <sup>-5</sup> <sup>c</sup>					
f <sub_bnz_phe< sub=""></sub_bnz_phe<>									0.87 <sup>b</sup>
f <sub>h2_phe</sub>									0.13 <sup>b</sup>
f <sub>ac_bnz</sub>									0.51 <sup>b</sup>
f <sub>h2_bnz</sub>									0.49 <sup>b</sup>
f <sub>ac_fua</sub>									0.82 <sup>d</sup>
f <sub>h2_fua</sub>									0.10 <sup>d</sup>
f <sub>ac_HMF</sub>									0.88 <sup>e</sup>
f <sub>h2_HMF</sub>									0.12 <sup>e</sup>

<sup>a</sup> Calculated/Estimated

<sup>c</sup> Raya et al. (2021)

<sup>e</sup> B. Liu et al. (2017)

<sup>g</sup> Brune et al. (1983)

<sup>b</sup> Fezzani and Ben Cheikh (2009)

<sup>d</sup> Li et al. (2023)

<sup>f</sup> Araya et al. (2000)

<sup>h</sup> Gąszczak et al. (2012)

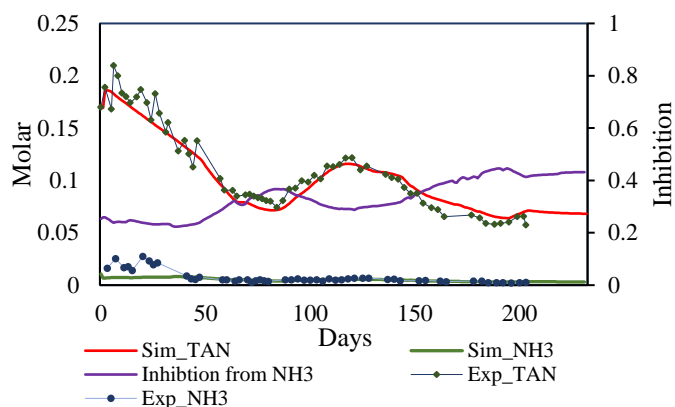


Fig. 2. Simulated total ammonia nitrogen (TAN) (red line) and free ammonia,  $\text{NH}_3$ , (green line) are plotted against experimental data (dots) for the HS-reactor. The inhibition of  $\text{NH}_3$  is also plotted, (purple line) where 0 = full inhibition and 1 = no inhibition.

Moreover, the model had difficulty when there were sharp changes in inflow. Simulated methane concentration is, on average, 67.3% in the last 100 days, close to the experimental methane concentration of 67.8% analyzed in that period.

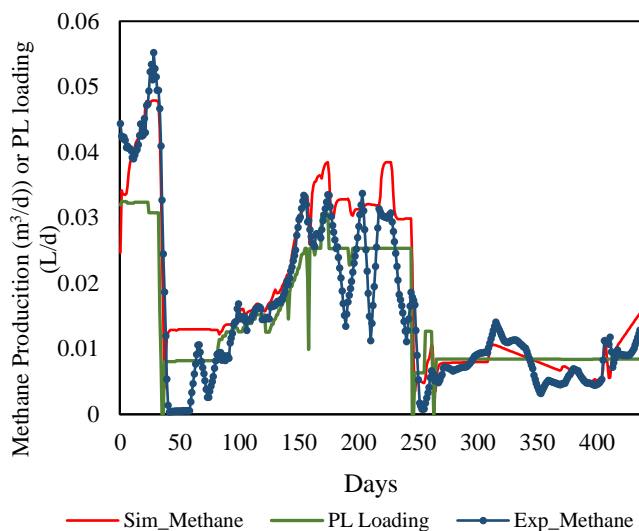
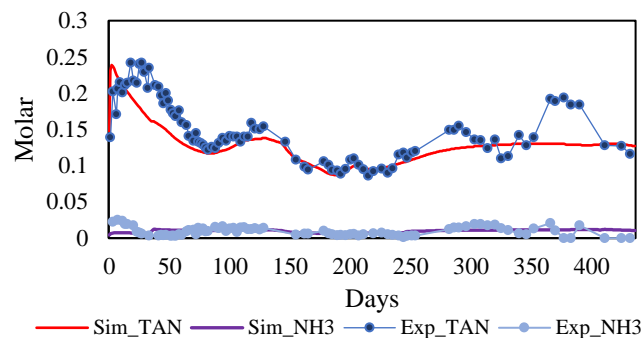
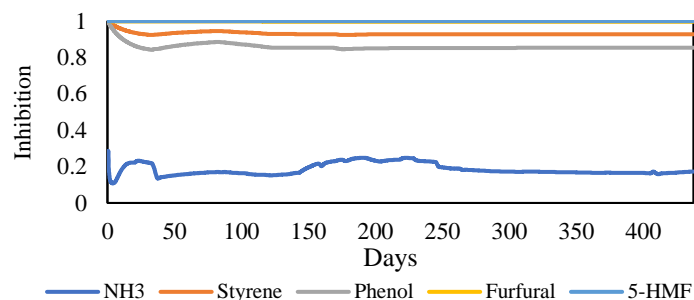


Fig. 3. Simulated (red line) and experimental methane production (black dots) of reactor treating hydrolyzed sludge (HS) and biosolid pyrolysis liquid (PL). The PL loading (green line) is added to visualize substrate load changes during the experiment.

Inorganic nitrogen and inhibitions of the HSPL-reactor are plotted in Fig. 4, where the main contributor to inhibition is  $\text{NH}_3$ . TAN is underestimated in the model until day 65; however, it is comparable to the experimental value until day 350, when the reactor effluent had an increase in TAN concentration. This effect might be due to substrate variations, such as more proteins entering the reactor or accumulation inside the reactor. Inhibition from  $\text{NH}_3$  was 0.14, 0.85 for phenol, and 0.93 for styrene, while furfural and HMF had no significant contribution (0 – 0.1%). Also, in this case,  $\text{NH}_3$  is underestimated in the first days, so inhibition was lower during that period.  $\text{NH}_3$  is correlated to pH, where ammonium and  $\text{NH}_3$  are in equilibrium, and an increase in pH shifts the equilibrium toward  $\text{NH}_3$ . pH was simulated to be 7.85, which is slightly higher than the average experimental pH (7.7).



— Sim\_TAN — Sim\_NH3 — Exp\_TAN — Exp\_NH3



— NH3 — Styrene — Phenol — Furfural — 5-HMF

Fig. 4. (Top figure) Simulated total ammonia nitrogen (TAN) (red) and free ammonia ( $\text{NH}_3$ ) (purple) are plotted against experimental data (dots) for the HSPL-reactor. (Bottom figure) The inhibition of  $\text{NH}_3$ , styrene, phenol, furfural, and 5-HMF are plotted where 0=full inhibition and 1=no inhibition.

### 3.3 Discussion

Previous studies simulating digesters fed with HS in ADM1 showed good fits with experimental data, but VFAs were the only parameter challenging to simulate (Donoso-Bravo et al., 2020; Flatabø and Bergland, 2022). Similar problems occurred in this simulation, where the experimental acetic acid concentration was 170% higher than the simulated values.

Another study has shown that effluent COD has been accurately predicted while methane production has been overestimated (Souza et al., 2013a). The current study indicates that simulated methane production was accurately predicted for HS-reactors with an average 10.1% overestimation and sCOD concentrations (not shown) in the effluent was 3.7% overestimated) while the tCOD concentration (not shown) in the effluent was 12.6% underestimated. For the HSPL-reactor, the methane production in the period after 266 days is 14.8% higher, but with significant deviations in the simulation, the simulated tCOD in the effluent (not shown) had an underestimation of 30.4%, and sCOD (not shown) had an underestimation of 26.5%. A previous study of HS in continuous systems with an over/underestimation of 15% was acceptable due to operational variability (Souza et al., 2013b). This study, therefore, shows that the simulation predicts methane production with acceptable accuracy for HS. For the simulation of HS-PL, methane production was better predicted at the end of the period but was not well predicted at high loadings. Souza et al. (2013a) previously reported that methane production deviates in response to low HRTs and consequent load changes. In this study, simulated methane production was not well predicted at low (16.2 days) HRTs,

the first 34 days and between 158 and 245 days, as seen in Fig. 5. However, at high HRT (low mass loadings), the simulation predicts the methane production accurately.

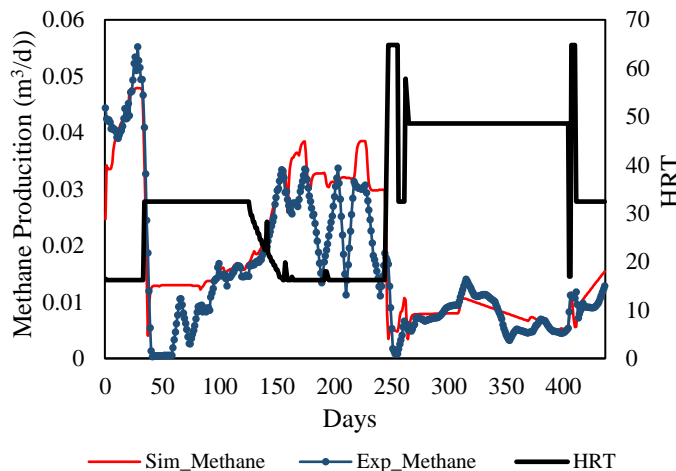


Fig. 5. Simulated (red) and experimental (blue) methane production compared to hydraulic retention time (HRT) (black line).

Considering the operating variability, the simulation's overestimation of 10.1% methane production for the HS-reactor is acceptable. The difference between simulated and experimental values is significantly higher for the HSPL-reactor. Methane production is still overestimated in the stable period with high HRT and low PL loading. The reason might be that the PL consists of more inhibitors than those accounted for in the modelling or that the inhibiting compounds have higher concentrations than the literature has suggested.

### 3.4 Inhibition

Phenols are found in agricultural and industrial wastes and are known to inhibit biodegradation, which makes biological processes difficult to occur (Hernandez and Edyvean, 2008). In AD, it has been indicated that the phenolic compounds interfere with the chain of reactions prior to methanogenesis. Therefore, hydrolysis and acetogenesis are inhibited more than methanogenesis (Hernandez and Edyvean, 2008). Literature suggests that there is some uncertainty regarding phenol methanization where data varies considerably, and some also report that methanization was not achieved (Hernandez and Edyvean, 2008). Another concern is the inhibition constant, which has varying data from 1.12 to 5 kg COD/m<sup>3</sup> (Blum and Speece, 1991; Hernandez and Edyvean, 2008; Raya et al., 2021). Therefore, there is some uncertainty regarding the inhibition constant ( $K_i$ ) and phenols degradation to methane. Styrene in typical AD reactors usually comes from synthetic monomers for plastic production. Fractions of styrene will volatilize, but some will be present in the liquid phase, which can inhibit microbes (Araya et al., 2000). Previous studies have reported styrene in PL (Kessas et al., 2021; Z. Liu et al., 2017); however, the current study's concentration is unknown, and data from the literature was used. Furfural and 5-HMF inhibition were not significant, which was expected because these inhibitors are mainly found in lignocellulosic material or low-temperature pyrolysis (Leng et al., 2021). Phenols and

inorganic nitrogen were expected to be high because of the lignin and protein content (Leng et al., 2021).

TAN (ammonium + NH<sub>3</sub>) is regarded as a nutrient for microbes, but too high concentrations (over 1700 mg/L) can lead to reactor failure (Yenigün and Demirel, 2013). However, microbes can acclimate to high TAN-concentrations when gradually exposed to higher loading over a long period. NH<sub>3</sub> is a potent inhibitor and is in equilibrium with ammonium which increases with a rise in either temperature or pH. According to a previous study of HS-PL, the inhibition from NH<sub>3</sub> was 0.19 at an organic loading rate PL of 0.41 kg tCOD/m<sup>3</sup>/d (Flatabø and Bergland, 2022). In this study, the average inhibition (0.14) is slightly higher than what Flatabø and Bergland (2022) reported but is in the range (0.126-0.268). However, the inhibition of NH<sub>3</sub> is correlated to the inflow of TAN, PL loading, HRT, and pH. Regarding pH, it was relatively stable during the entire period which means that pH did not significantly shift the equilibrium between ammonium and NH<sub>3</sub>. Therefore, this is not considered a major contributor to this simulation compared to the actual TAN concentration loaded. From day 143 to 246, there is less inhibition (see Fig. 4), which can be explained by the lower TAN inflow (average 0.067 M) and the low HRT. However, in the initial period, there was a high TAN (0.1464 M) with low HRT and less inhibition. Based on those findings, it can be seen that low HRT is beneficial for reducing the inhibition of NH<sub>3</sub>. A higher HRT allows more proteins to degrade to TAN. Another possibility is that a low HRT restrains the contact time between microbes and compounds, making the inhibitor less potent. Moreover, the lower HRT gives a more unstable digestion.

Moreover, this article does not take into account the adsorption mechanisms of the different compounds onto the sludge. Phenols can adsorb onto the sludge with a saturation level of 800-1600 mg/L (Hernandez and Edyvean, 2008). Also, microbial adaptation can reduce the effect inhibitors have on methane production over time, which is not taken into account in the model (Donoso-Bravo et al., 2022). Microbes will be selected in continuous reactors based on their adaptability to the substrate, making microbial adaptation an essential factor in the model. The inhibition data also differ from a batch reactor to a CSTR; for this study, the data is not calibrated to a semi-continuous system. Previously, Li et al. (2023) found that  $K_i$  was 2.47 kg COD/m<sup>3</sup> for batch and 6.05 kg COD/m<sup>3</sup> for a continuous system where some microbial kinetics were also changed. This suggests that inhibition and kinetic parameters could be calibrated for a better fit in the model.

### 3.5 Effect of Pyrolysis Liquid addition

The effects of PL addition were evaluated on the methane production of the simulated reactor with HS-PL and the reactor with the same inflow of HS but without PL (see Fig. 6). The difference is noticed as the additional methane production from PL. Based on the results, PL has a positive contribution even though it brings several inhibitors. However, at high PL loadings, it looks like the increased inhibition may lead to reduced methane production.

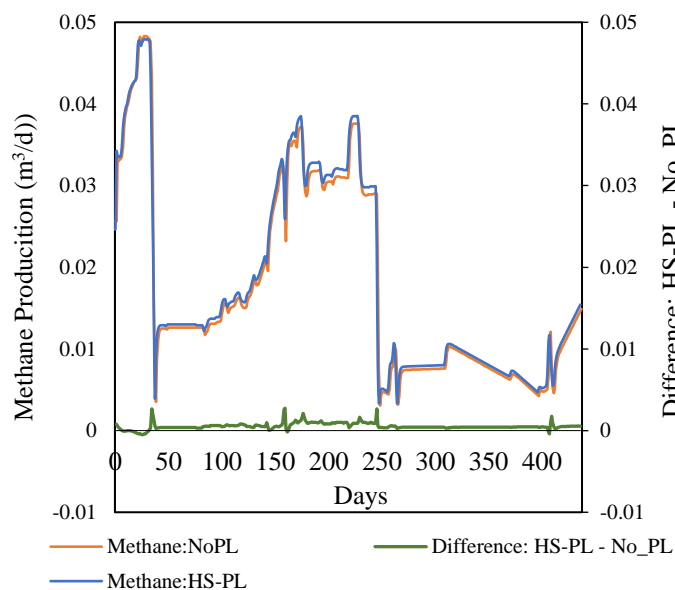


Fig. 6. Simulation of methane production of hydrolyzed sludge with (blue line) or without PL (orange line). The green line shows the difference in methane production between HS with or without PL.

Tab. 4 summarizes the most important parameters and how PL affected them. According to the simulation, PL enhances inhibition but also increases methane production. The methane partial pressure in the biogas and the reactor pH also increased slightly.

Table 4: Average data on PL's influence on AD.

Parameter	PL's influence on AD	St. dev (%)
Methane production	+4.3%	3.0
Inhibition	+31.2%	7.2
pH	+0.8 %	0.9
Methane partial pressure	+1.3%	0.6

### 3. CONCLUSIONS

This study aimed to investigate the effect of PL in co-digestion with HS in an extended ADM1 simulation. The results showed that the model predicted AD of HS with a 10.1% overestimation and that the model did not respond well to sharp load changes. For the HS-PL simulation, the model overpredicts methane production significantly, and the results suggest that there are more inhibitors in the PL than those implemented in the model. According to simulation results, ammonia, phenol, and styrene contributed to most inhibition and increased inhibition by 31%. However, due to the additional COD in the PL, there was additional methane production of 4.3%. Results showed that PL has a positive impact at low loadings. For future work, it is recommended that more studies be conducted on the inhibitor and implementation of microbial adaptation in modelling.

### ACKNOWLEDGEMENTS

The authors would like to thank the NORPART project for financing the expenses for presenting this study at the SIMS

EUROSIM 2024. This study was funded by the University of South-Eastern Norway (USN). Lindum AS and VOW ASA provided substrate and PL for the study.

### REFERENCES

- Araya, P., Chamy, R., Mota, M., and Alves, M. (2000). Biodegradability and toxicity of styrene in the anaerobic digestion process. *Biotechnology letters*, 22, 1477-1481.
- Arnold, M., Reittu, A., Von Wright, A., Martikainen, P. J., and Suihko, M. L. (1997). Bacterial degradation of styrene in waste gases using a peat filter. *Applied Microbiology and Biotechnology*, 48(6), 738-744. doi:10.1007/s002530051126
- Batstone, D. J., Keller, J., Angelidaki, I., Kalyuzhnyi, S. V., Pavlostathis, S. G., Rozzi, A., Sanders, W. T. M., Siegrist, H., and Vavilin, V. A. (2002). The IWA Anaerobic Digestion Model No 1 (ADM1). *Water Science and Technology*, 45(10), 65-73. doi:10.2166/wst.2002.0292
- Bergland, W. H., Dinamarca, C., Toradzadegan, M., Nordgård, A. S. R., Bakke, I., and Bakke, R. (2015). High rate manure supernatant digestion. *Water Research*, 76, 1-9. doi:10.1016/j.watres.2015.02.051
- Blum, D. J. W., and Speece, R. (1991). A Database of Chemical Toxicity to Environmental Bacteria and Its Use in Interspecies Comparisons and Correlations. *Research Journal of the Water Pollution Control Federation*, 63. doi:10.2307/25043983
- Brune, G., Schoberth, S. M., and Sahn, H. (1983). Growth of a Strictly Anaerobic Bacterium on Furfural (2-Furaldehyde). *Appl Environ Microbiol*, 46(5), 1187-1192. doi:10.1128/AEM.46.5.1187-1192.1983
- Donoso-Bravo, A., Olivares, D., Lesty, Y., and Bossche, H. V. (2020). Exploitation of the ADM1 in a XXI century wastewater resource recovery facility (WRRF): The case of codigestion and thermal hydrolysis. *Water Research*, 175, 115654. doi:10.1016/j.watres.2020.115654
- Donoso-Bravo, A., Sadino-Riquelme, M. C., Valdebenito-Rolack, E., Paulet, D., Gómez, D., and Hansen, F. (2022). Comprehensive ADM1 Extensions to Tackle Some Operational and Metabolic Aspects in Anaerobic Digestion. *Microorganisms*, 10(5), 948. doi:10.3390/microorganisms10050948
- Feng, Q. J., and Lin, Y. Q. (2017). Integrated processes of anaerobic digestion and pyrolysis for higher bioenergy recovery from lignocellulosic biomass: A brief review. *Renewable and Sustainable Energy Reviews*, 77, 1272-1287. doi:10.1016/j.rser.2017.03.022
- Fezzani, B., and Ben Cheikh, R. (2009). Extension of the anaerobic digestion model No. 1 (ADM1) to include phenol compounds biodegradation processes for simulating the anaerobic co-digestion of olive mill wastes at mesophilic temperature. *Journal of Hazardous Materials*, 172(2-3), 1430-1438. doi:10.1016/j.jhazmat.2009.08.017

- Flatabø, G. Ø., and Bergland, W. H. (2022, 2022). Anaerobic Co-Digestion of Products from Biosolids Pyrolysis – Implementation in ADM1.
- Flatabø, G. Ø., Cornelissen, G., Carlsson, P., Nilsen, P. J., Tapasvi, D., Bergland, W. H., and Sørmo, E. (2023). Industrially relevant pyrolysis of diverse contaminated organic wastes: Gas compositions and emissions to air. *Journal of cleaner production*, 423, 138777. doi:10.1016/j.jclepro.2023.138777
- Flatabø, G. Ø., Indrebø, T. S., Svennevik, O. K., Ahmed, B., Nilsen, P. J., and Bergland, W. H. (2024). Anaerobic Co-Digestion of Sewage Sludge and its Pyrolysis Condensate: Implications for Methane Production and Filtrate Water Quality. *Heliyon*. doi:10.2139/ssrn.4829930 (Accepted)
- Gąszczak, A., Bartelmus, G., and Greń, I. (2012). Kinetics of styrene biodegradation by *Pseudomonas* sp. E-93486. *Applied Microbiology and Biotechnology*, 93(2), 565-573.
- Giwa, A. S., Xu, H., Chang, F. M., Zhang, X. Y., Ali, N., Yuan, J., and Wang, K. J. (2019). Pyrolysis coupled anaerobic digestion process for food waste and recalcitrant residues: Fundamentals, challenges, and considerations. *Energy Science and Engineering*, 7(6), 2250-2264. doi:10.1002/ese3.503
- Han, D., Lee, C.-Y., Chang, S. W., and Kim, D.-J. (2017). Enhanced methane production and wastewater sludge stabilization of a continuous full scale thermal pretreatment and thermophilic anaerobic digestion. *Bioresource Technology*, 245, 1162-1167. doi:10.1016/j.biortech.2017.08.108
- Hernandez, J. E., and Edyvean, R. G. J. (2008). Inhibition of biogas production and biodegradability by substituted phenolic compounds in anaerobic sludge. *Journal of Hazardous Materials*, 160(1), 20-28. doi:10.1016/j.jhazmat.2008.02.075
- Hubner, T., and Mumme, J. (2015). Integration of pyrolysis and anaerobic digestion - Use of aqueous liquor from digestate pyrolysis for biogas production. *Bioresource Technology*, 183, 86-92. doi:10.1016/j.biortech.2015.02.037
- Kessas, S. A., Esteves, T., and Hemati, M. (2021). Products Distribution During Sewage Sludge Pyrolysis in a Sand and Olivine Fluidized Bed Reactor: Comparison with Woody Waste. *Waste and Biomass Valorization*, 12(6), 3459-3484. doi:10.1007/s12649-020-01209-9
- Leng, L. J., Yang, L. H., Chen, J., Hu, Y. B., Li, H. L., Li, H., Jiang, S. J., Peng, H. Y., Yuan, X. Z., and Huang, H. J. (2021). Valorization of the aqueous phase produced from wet and dry thermochemical processing biomass: A review. *Journal of cleaner production*, 294, Article 126238. doi:10.1016/j.jclepro.2021.126238
- Li, P., Wei, X., Wang, M., Liu, D., Liu, J., Pei, Z., Shi, F., Wang, S., Zuo, X., Li, D., Yu, H., Zhang, N., Yu, Q., and Luo, Y. (2023). Simulation of anaerobic co-digestion of steam explosion pulping wastewater with cattle manure: Focusing on degradation and inhibition of furfural. *Bioresource Technology*, 380, 129086. doi:10.1016/j.biortech.2023.129086
- Liu, B., Ngo, V. A., Terashima, M., and Yasui, H. (2017). Anaerobic treatment of hydrothermally solubilised sugarcane bagasse and its kinetic modelling. *Bioresource Technology*, 234, 253-263. doi:10.1016/j.biortech.2017.03.024
- Liu, Z., McNamara, P., and Zitomer, D. (2017). Autocatalytic Pyrolysis of Wastewater Biosolids for Product Upgrading. *Environmental Science and Technology*, 51(17), 9808-9816. doi:10.1021/acs.est.7b02913
- Raya, D., Ghimire, N., Flatabø, G. Ø., and Bergland, W. H. (2021). Anaerobic Digestion of Aqueous Pyrolysis Liquid in ADM1. doi:10.3384/ecp21185458
- Seyedi, S., Venkiteshwaran, K., Benn, N., and Zitomer, D. (2020). Inhibition during Anaerobic Co-Digestion of Aqueous Pyrolysis Liquid from Wastewater Solids and Synthetic Primary Sludge. *Sustainability*, 12(8), Article 3441. doi:10.3390/su12083441
- Seyedi, S., Venkiteshwaran, K., and Zitomer, D. (2019). Toxicity of Various Pyrolysis Liquids From Biosolids on Methane Production Yield. *Frontiers in Energy Research*, 7, Article 5. doi:10.3389/fenrg.2019.00005
- Souza, T. S. O., Carvajal, A., Donoso-Bravo, A., Peña, M., and Fdz-Polanco, F. (2013a). ADM1 calibration using BMP tests for modeling the effect of autohydrolysis pretreatment on the performance of continuous sludge digesters. *Water Research*, 47(9), 3244-3254. doi:10.1016/j.watres.2013.03.041
- Souza, T. S. O., Ferreira, L. C., Sapkaite, I., Pérez-Elvira, S. I., and Fdz-Polanco, F. (2013b). Thermal pretreatment and hydraulic retention time in continuous digesters fed with sewage sludge: Assessment using the ADM1. *Bioresource Technology*, 148, 317-324. doi:10.1016/j.biortech.2013.08.161
- Tayibi, S., Monlau, F., Marias, F., Cazaudehore, G., Fayoud, N.-E., Oukarroum, A., Zeroual, Y., and Barakat, A. (2021). Coupling anaerobic digestion and pyrolysis processes for maximizing energy recovery and soil preservation according to the circular economy concept. *Journal of Environmental Management*, 279, 111632. doi:10.1016/j.jenvman.2020.111632
- Yenigün, O., and Demirel, B. (2013). Ammonia inhibition in anaerobic digestion: A review. *Process Biochemistry*, 48(5), 901-911. doi:10.1016/j.procbio.2013.04.012